Observation of a linear dependence of the frequency splitting between GaAs and AlAs optical surface phonons as a function of Al concentration in $Al_xGa_{1-x}As$

J.-L. Guyaux, P. A. Thiry, R. Sporken, and R. Caudano
Laboratoire Interdisciplinaire de Spectroscopie Electronique, Institute for Studies in Interface Sciences, Facultés Universitaires Notre-Dame de la Paix, 61 rue de Bruxelles, B-5000 Namur, Belgium

Ph. Lambin
Laboratoire de Physique du Solide, Institute for Studies in Interface Sciences, Facultés Universitaires Notre-Dame de la Paix, 61 rue de Bruxelles, B-5000 Namur, Belgium
(Received 29 March 1993)

In this paper, we report on the high-resolution electron-energy-loss spectroscopy study of high-quality $Al_xGa_{1-x}As$ ternary alloys in the whole range of Al concentration, from $x=0$ to 1. The ternary alloys have been grown by molecular-beam epitaxy and analyzed in the same ultrahigh-vacuum (UHV) environment. For intermediate Al concentrations we observe two long-wavelength surface phonons which can be associated with the vibrations of Ga or Al atoms against As atoms, respectively. Precise values of the frequencies of these two modes versus the Al concentration are deduced from a semitheoretical fit of the spectra and compared with the theoretical model based on the coherent-potential approximation. The surface-phonon frequency splitting provides an alternative way of determining the aluminum concentration in such ternary alloys. The intensities of both losses are considered in the framework of the dielectric theory and some conclusions are drawn for the oscillator strengths of the two surface modes.

I. INTRODUCTION

In recent years, mixed semiconductor crystals have been studied extensively both experimentally and theoretically, because they provide new materials with tailored properties, such as adjustable lattice parameters or band gaps, intermediate between the ones of the pure crystals. Among the III-V ternary semiconductors, $Al_xGa_{1-x}As$ alloys play an important role, especially for close lattice-matched heterojunctions in optoelectronic devices. The electronic properties of these materials are well understood. However, because of the intrinsic mixing of elements that occur, their structural properties still lack a precise description. Some of these structural properties can be revealed experimentally through an analysis of the vibrational eigenmodes.

This is the reason why considerable work has been devoted to understanding the long-wavelength phonon-dispersion behavior versus the Al molar fraction in $Al_xGa_{1-x}As$ ternaries. Such an investigation has to be carried out in a range of wavelengths long enough to avoid the influence of the local arrangement of the elements and reveal a general picture corresponding to the average distribution of III-V atoms in the crystal. In this respect, optical spectroscopies are appropriate and they have already delivered many significant results.

The frequencies of the longitudinal-(LO) and transverse-(TO) optical modes of $Al_xGa_{1-x}As$ mixed crystal have been studied by Ilegems and Pearson[1] from the Kramers-Kronig analysis of infrared reflectance spectra. Similar studies have been performed by Tsu, Kawamura, and Esaki[2], and Abstreiter *et al.*[3] using Raman spectroscopy. More recently, Jusserand and Sapriel[4] repeated the measurements of the LO and TO modes *versus* the Al concentration and analyzed in detail the line-shape asymmetry of these modes in terms of defects and anharmonicity. The dispersive character of the phonon branches of $Al_xGa_{1-x}As$ disordered material has been observed by Raman spectroscopy on $Al_xGa_{1-x}As/GaAs$ superlattices.[5] Optical properties of $Al_xGa_{1-x}As$ from the visible to near-ultraviolet frequency range (1.5–6 eV) for Al concentrations between $x=0$ and 0.8 have been obtained by Aspnes *et al.*[6] using optical reflection techniques.

The long-wavelength vibrational behavior of *n*-doped $Al_xGa_{1-x}As$ has also been studied by Raman spectroscopy.[7,8] Besides the phonon line frequencies, such material exhibits a free-carrier plasmon signature. The LO phonons and the free-carrier plasmon are coupled by the interaction of the electric dipole moment induced by the relative displacement of the ions and the electric field associated with the free carriers. The presence of free carriers excludes the possibility of determining correctly the LO and TO frequencies without accounting for the coupling that shifts dramatically the phonon bands at high electron concentration. Due to this fact, the use of undoped mixed crystals for studying long-wavelength phonons is more appropriate.

For a detailed review of the theoretical models describing the vibrational structure of mixed crystals, we refer to the review papers of Chang and Mitra[9] and Barker and Sievers.[10] A comprehensive theory has been constructed

using the coherent potential approximation (CPA) model developed by Bonneville.[11] More recently, Baroni, de Gironcoli, and Giannozzi[12] have presented an *ab initio* model by which they determined the dispersion of the phonon branches in thin AlAs and GaAs films allowing us to deduce long-wavelength optical phonons. The study of the ternary alloys regained interest since the discovery of the confined LO phonons in superlattices which are due to mixing occurring at the interface.

In this paper, we report on measurements of the long-wavelength surface optical phonons in $Al_xGa_{1-x}As$ films grown by molecular-beam epitaxy (MBE) in the whole range of composition ($0<x<1$). The measurements have been carried out by high-resolution electron-energy-loss spectroscopy (HREELS) which has proved to be a well dedicated tool to study macroscopic excitations at a solid surface. At the surface of polar semiconductors, long-wavelength optical surface phonons, often called Fuchs-Kliewer (FK) modes, develop a long-range polarization field. This polarization field can couple to an incident charged particle that can lose or gain energy by creating or annihilating quanta of such phonons.[13] The frequency associated to the FK mode falls inside the LO and TO gap.

In mixed crystals, the dependence of the optical properties on the atomic composition can be twofold: the one-mode or two-mode behavior. In the one-mode behavior, the frequencies of each of the long-wavelength ($\mathbf{k}\cong\mathbf{0}$) transverse- and longitudinal-optical modes vary from the mode frequency of one end member to that of the other one. On the contrary, the two-mode behavior exhibits for an intermediate mixing ratio two sets of phonon frequencies appearing close to those of the end members. The strength of one mode seems to be proportional to the mole fraction of the corresponding component.[9] Some mixed crystals show the two-mode behavior over some part of the composition range and one-mode behavior over another part. This is usually the case for the III-V semiconductor ternary alloys.

Although this cannot be considered as a general law, it is observed in most cases that ionic compounds exhibit a one-mode behavior whereas covalent materials show a two-mode behavior. In $Al_xGa_{1-x}As$, the long-wavelength optical phonons display a two-mode behavior throughout the entire composition range. There are thus two pairs of TO and LO modes: one being assigned to a GaAs-like mode and the other to an AlAs-like mode. GaAs-like mode frequencies approach those of the GaAs phonons when the aluminum molar fraction (x) reaches zero, while AlAs-like modes converge to the pure AlAs values when x approaches one. Two surface phonons can be expected, one associated to the AlAs-like bulk branches and the other one to the GaAs-like branches. The collection of HREELS spectra recorded on different samples allows us to represent the FK mode frequency versus the aluminum concentration. The most important result of this paper is that the frequency splitting between the two surface phonons exhibits a nearly linear behavior throughout the entire range of aluminum concentration. This parameter provides a means of determining the aluminum concentration of unknown $Al_xGa_{1-x}As$ mixed crystals.

In a previous set of experiments, Thiry *et al.*[14] have carried out a HREELS study of $Al_xGa_{1-x}As$ films and reported the qualitative observation of the two FK phonon branches. However, in that case, because the samples had to be transferred through air, the exact stoichiometry of the alloys was uncertain after the necessary cleaning treatment that involved annealing and ion sputtering. The originality of the study presented here is that the $Al_xGa_{1-x}As$ samples were grown *in situ,* in a MBE chamber interconnected to the HREELS spectrometer. By this, high-quality material could be available for HREELS study. Furthermore, the exact alloy composition could be monitored by reflection high-energy electron diffraction (RHEED) during growth so that a quantitative interpretation of the HREELS data was feasible.

II. EXPERIMENT

The experiments reported here were carried out in a system combining a high-resolution electron-energy-loss spectrometer and a molecular-beam-epitaxy reactor. The whole system is kept under ultrahigh vacuum (UHV) conditions with a residual pressure below 10^{-8} Pa in the spectrometer and the growth chamber and 10^{-7} Pa in the preparation chamber connecting these two. The MBE chamber is equipped with three effusion cells for Al, Ga, and As and with a 10-keV RHEED system. Due to the reduced size of the sample (<1 cm^2) imposed by the spectrometer, no azimuthal rotation was needed during the growth.

$\langle 100\rangle$-oriented gallium arsenide wafers are used as substrates. After degreasing and etching in a H_2SO_4:H_2O_2:H_2O(5:1:1) solution, the wafer is glued with liquid indium on a molybdenum sample holder and introduced in the preparation chamber via a load-lock system. A moderate heating under arsenic flux above 580 °C allows us to remove the oxide layer formed after the rinsing step. The temperature is measured and regulated with an infrared pyrometer. The desorption temperature of gallium oxide (580 °C),[15] as well as the surface phase transition between the two arsenic-rich reconstructions $c(2\times8)$ to $c(4\times4)$ were used to calibrate the pyrometer.

A 2000-Å-thick buffer layer of GaAs is deposited on the substrate before starting the $Al_xGa_{1-x}As$ alloy growth. Ternary compounds are grown at 580 °C as in the case of the buffer layer. With a suitable choice of gallium and aluminum cell temperatures, the whole range of concentration of the ternary alloy is accessible. The aluminum concentration is determined by recording the RHEED oscillations.[16]

After growth, the sample is transferred under UHV into the analysis chamber. The electron spectrometer (SEDRA, ISA Riber) is equipped with two hemispherical capacitors as monochromator and analyzer. The HREELS spectra have been recorded in the dipole scattering configuration (specular geometry). Under these conditions, the long-range nature of the Coulomb field accompanying the moving electron implies that the probing electrons interact principally with long-

wavelength excitations ($\mathbf{k} \cong \mathbf{0}$). The combination of MBE and HREELS allows a perfectly consistent set of measurements where the sample remains under UHV conditions without exposure to any contaminants other than the residual gases of the UHV chamber. The spectra recorded immediately after the growth did not show any hydrocarbon or oxide contaminant vibrations at the detection limit of HREELS (<0.01 monolayer). The resolution of the HREELS spectra reported here was found to be within the range of 48–56 cm^{-1} as measured from the full width at half maximum (FWHM) of the elastic peak. The impact energy of the incident electron beam used in the present study is of the order of 3 eV. All the HREELS spectra have been recorded at room temperature.

III. RESULTS AND DISCUSSIONS

Figure 1 shows a typical spectrum recorded on an $Al_xGa_{1-x}As$ ternary alloy where the aluminum atomic concentration was 0.55. The spectrum has been recorded in specular geometry $\theta_i = \theta_r = 45°$ with respect to the surface normal and with an incident electron impact energy (E_0) of 2.91 eV as measured by scanning the energy-loss spectrum up to the cutoff. A low impact energy (E_0) ensures a high dipole cross section since the loss probability is proportional to $E_0^{-(1/2)}$. At such an energy the angular aperture of the dipole lobe $\hbar\omega/2E_0$ ($\hbar\omega$ is the energy lost by the moving electrons) is still small as compared with the monochromator aperture (Ψ_a).[17]

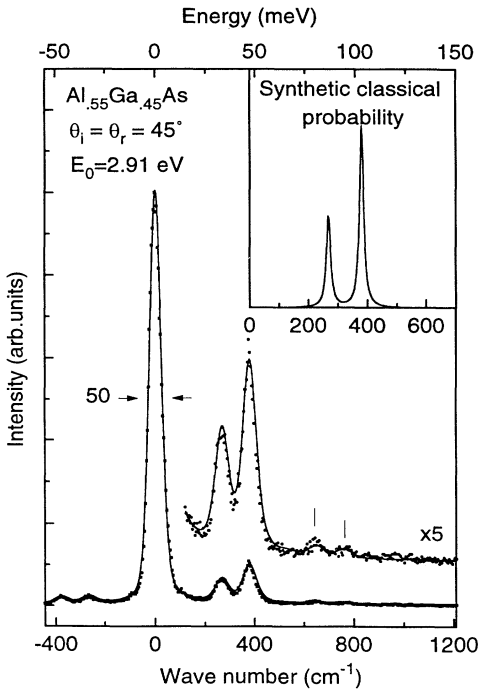

FIG. 1. Typical HREELS spectrum recorded on a $Al_{0.55}Ga_{0.45}As$ mixed crystal. The inset displays the synthetic first-order loss probability which by convolution with the quantum-mechanical loss distribution gives the complete semitheoretical spectrum solid line superimposed to the experimental data.

In the spectrum of Fig. 1, we observe characteristic energy loss and gain features symmetrically located on both sides of the elastic peak. The Boltzmann factor $\exp[-(\hbar\omega/kT)]$ reduces the gain peak intensity in comparison to the loss part of the spectrum. In the loss region, we distinguish two main peaks attributed to two long-wavelength surface phonons of the mixed crystal. A simple consideration based on the lighter mass of the aluminum atom allows us to predict that the higher frequency peak is related to an AlAs-like phonon. Three much weaker loss features are observed at higher frequencies. They can be attributed to double scattering, i.e., incoming electrons loosing energy by creating two phonons of the same or different type.

To determine accurately the frequency of the two main peaks, we adopt a semitheoretical way. First, we construct a so-called "synthetic first-order classical probability" which is, in fact, the frequency resolved energy-loss spectrum, as a sum of Lorentzian line shapes to simulate the two AlAs- and GaAs-like surface losses (see the insert in Fig. 1). This can be justified by the fact that the surface loss function is $(1/\omega)\mathrm{Im}\{-1/[\varepsilon(\omega)+1]\}$, where $\varepsilon(\omega)$ is the dielectric function of the bulk material described by a double-oscillator Lorentzian formula. Some algebra shows that the loss function can be written, in the case of small oscillator damping as a sum of two δ functions which in the simulation can be replaced by Lorentzians. The second step constructs the quantum-mechanical loss distribution at temperature T which accounts for multiple excitation processes.[18] After convolution with the experimental response function (typically the elastic peak shape), the semitheoretical spectrum is compared with the experimental one. This set of procedures is included in an adjusting routine, where the adjustable parameters are the peak positions and intensities. Convergence to the satisfactory parameters is ensured by the minimization of the least-squares difference of both spectra. Figure 1 shows the semitheoretical spectrum superimposed on the experimental one. With this procedure we estimate the peak position with a precision of the order of 1 cm^{-1}.

Figure 2 displays a panel of HREELS spectra recorded on $Al_xGa_{1-x}As$ mixed crystals with different aluminum concentrations. These spectra have been normalized so as to present the same integral and the energy resolution measured as the FWHM of the quasi-elastic peak is within 48 and 54 cm^{-1} in the whole range of concentration. One can distinguish at extreme concentrations ($x=0$ and 1) the pure crystal vibration modes of GaAs and AlAs, respectively. These spectra exhibit a strong loss peak signature of one surface optical phonon. The corresponding peaks are at 288 cm^{-1} (GaAs) and 395 cm^{-1} (AlAs). In the intermediate mixing ratio, two lines are observed at frequencies close to the pure materials loss peaks and are assigned to the Ga (respectively, Al) As-like modes. Figure 3 presents the dispersion curve of

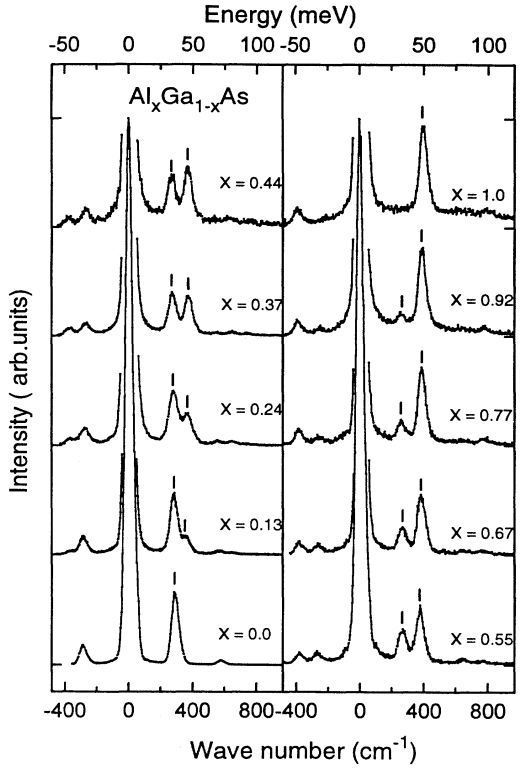

FIG. 2. Synoptic panel of the spectra recorded on the $Al_xGa_{1-x}As$ mixed crystals in the whole range of Al concentration. The energy resolution varied between 45 and 52 cm^{-1} as measured from the FWHM of the elastic peak.

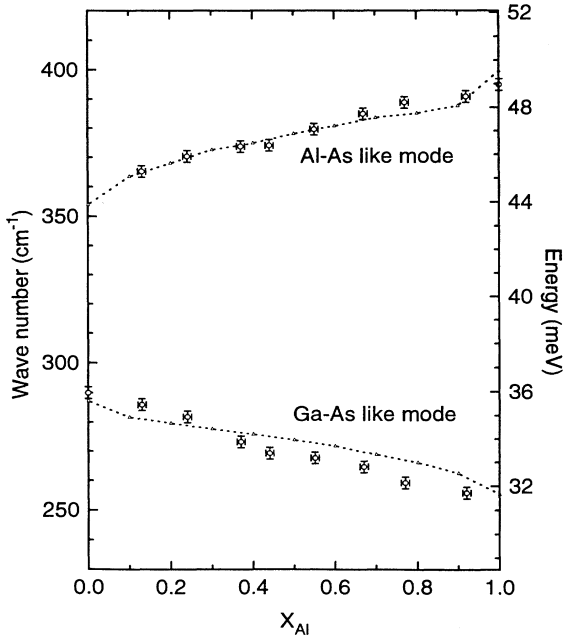

FIG. 3. Energy of the two optical surface phonons determined by the semitheoretical treatment vs the molar fraction of aluminum in $Al_xGa_{1-x}As$ mixed crystals. The dashed line represents the results of the CPA model.

the two surface phonons versus the Al concentration, determined by the semitheoretical way described above. The general tendency of the two lines is a downward shift from 295 to 250 cm^{-1} (395 to 360 cm^{-1}) of the surface loss frequency when the foreign atom concentration in the host crystal is increased. The high dilution limits ($x=0$ and 1) have been determined by linear least-squares fit for the GaAs-like (AlAs-like) branch when Al (Ga) concentration is increased. At the dilution limit, both branches converge to their respective impurity modes. When x approaches zero, the AlAs-like branch converges to a frequency well above the optical branches of the pure GaAs crystal. This frequency corresponds to the vibration of an isolated Al atom in the GaAs bulk material and is called an impurity "local" mode. The estimated value of this mode is 360 cm^{-1} which is not very far from 362 cm^{-1} determined by Raman spectroscopy.[19] On the other hand, when x approaches one, the GaAs-like branch converges to a frequency value in the gap between the optical and acoustic branches of the AlAs pure crystal; this is the so-called impurity "gap" mode. The value extrapolated from the HREELS surface phonon band is 250 cm^{-1} which again is very close to the value of 252 cm^{-1} measured by Raman spectroscopy.[1] The existence of these local and gap impurity modes is a necessary condition for having a two-mode behavior. The diatomic linear chain model proposed by Mazur *et al.*[20] gives a mass criterion to decide whether such a gap or local mode exists. It follows from this model that when the foreign atom replaces one of the lightest atoms of a diatomic host crystal such an impurity mode exists and can be of two kinds: if the impurity mass is lower than that of the replaced atom, a local mode is expected whereas if the impurity mass is between the masses of the two host crystal atoms, a gap mode is predicted.

Figure 4 displays the LO- and TO-phonon branches of the AlA-s and GaAs-like modes calculated by Bonneville[11] using the CPA (solid lines). Let us remark that for both modes, the longitudinal and transverse frequencies vary nearly linearly when $0.1 \leq x \leq 0.9$, but one observes a rapid decrease of the longitudinal-transverse (LT) splitting for x in the ranges 0–0.1 and 0.9–1, for the pure crystal modes as well as for the impurity modes. The data of Fig. 4 are not directly comparable with our results and need some treatment. From the two sets of LO and TO phonons calculated by the CPA model, it is straightforward to determine the dielectric function of the ternary alloys using the equation

$$\varepsilon(\omega)=\varepsilon_\infty \sum_{i=1,2} \frac{\omega_{\mathrm{LO}i}^2-\omega^2}{\omega_{\mathrm{TO}i}^2-\omega^2} , \tag{1}$$

where ε_∞ is the square of the refraction index. For the ternary alloy, we assume a linear dependence of ε_∞ (Ref. 21) with the aluminum concentration from the two end members high-frequency dielectric constant.[22]

As it follows from electromagnetism theory that the matching of the Maxwell equations at the interface between two semi-infinite dielectric media leads to the compatibility equation

$$\varepsilon_1(\omega)+\varepsilon_2(\omega)=0 , \tag{2}$$

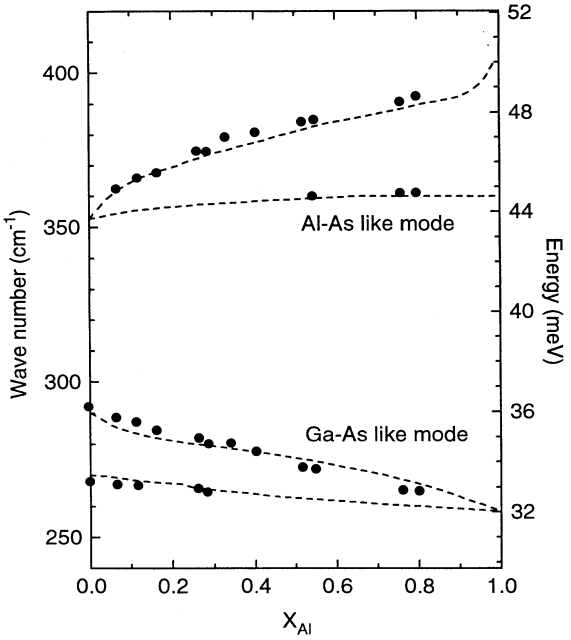

FIG. 4. The dashed line is the result of the CPA model of Bonneville (Ref. 11). The dots represent the experimental data obtained by Raman spectroscopy (Ref. 4).

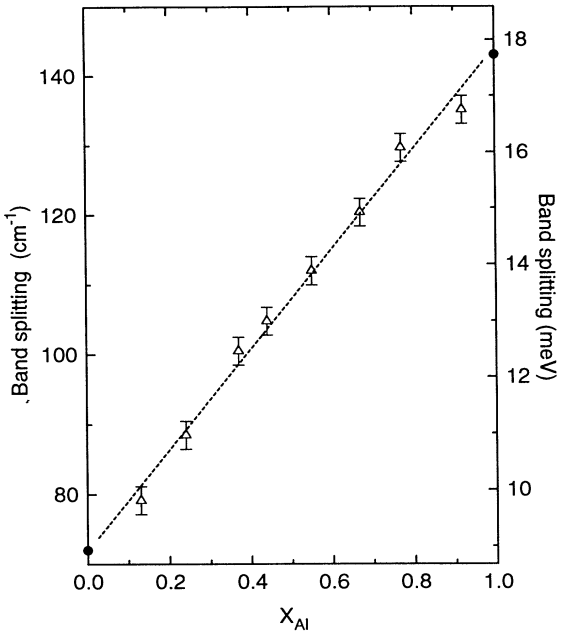

FIG. 5. Optical surface-phonon splitting. The values at $x=0$ or 1 are determined as the difference between the FK frequency of the pure GaAs or AlAs and the local or gap impurity mode found in the literature.

where ε_1 and ε_2 are the dielectric functions of the two media. Taking ε_1 as the dielectric function of $Al_xGa_{1-x}As$ as cast in Eq. (1) and $\varepsilon_2=1$ as the vacuum permittivity, the zeros of Eq. (2) give the optical surface mode frequencies of the ternary alloys. The results of this calculation were represented as dashed lines on Fig. 3. Let us first compare these theoretical results with our HREELS measurements for the AlAs mode. This mode exhibits a downward shift (4 cm^{-1}) when the Al concentration varies from 1.0 to 0.9. This shift is two times smaller than predicted by the theory. For the intermediate concentration, the theoretical branch fits quite well the experimental one and in the dilution limit, i.e., near the impurity local mode, we can extrapolate a downward shift similar to the one predicted by Bonneville's model. Although the AlAs-like FK branch predicted by the CPA theory is fairly well reproduced by the experimental data, the GaAs-like mode exhibits some discrepancy. Indeed, the theoretical calculation predicts a significant downward shift in the range between 0–0.1 followed by a linear behavior between 0.1–0.9 with a smaller slope. On the other hand, if the experimental GaAs-like branch shows a downward shift close to $x=0$, it is not so steep as predicted by the CPA model. The slope of the experimental branch for intermediate concentrations is more pronounced in the case of the experiment. Similar observations can be made on the Raman measurements done by Jusserand and Sapriel[4] (see Fig. 4) which show approximately the same behavior, i.e., a good agreement in the case of AlAs-like branch and some deviation for the GaAs-like branch.

Figure 5 displays the frequency difference between the two surface modes versus the aluminum concentration. As a consequence of the repulsion of the GaAs- and AlAs-like branches when x varies from zero to one (Fig. 3), the splitting of the two surface-phonon bands increases with Al concentration, from 75 cm^{-1} at $x=0$ to 140 cm^{-1} at $x=1$. We point out that at the extreme concentrations ($x=0$ or 1) the splitting has been determined as the difference between the FK frequency modes of the

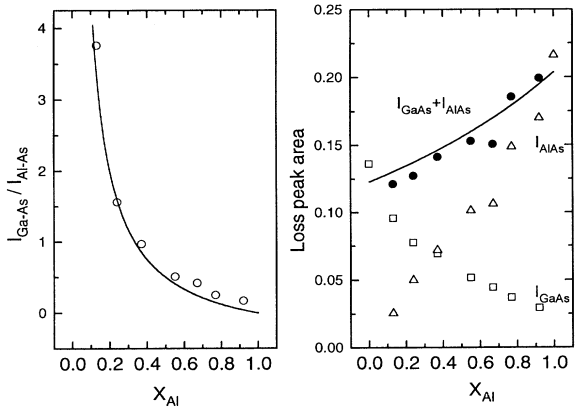

FIG. 6. Left panel: intensity ratio of the two main loss peaks vs the Al concentration. Right panel: intensities of the two main peaks. Intensities are determined by a semitheoretical fit of the normalized spectra. Open squares and triangles represent the GaAs- and AlAs-like peak areas, respectively. Filled circles represent the total loss area, i.e., the sum of the two loss peak areas.

pure materials (GaAs or AlAs) and the impurity (local or gap) mode frequencies found in the literature.[19,1] From pure GaAs to pure AlAs, the surface FK splitting varies quasilinearly with the aluminum concentration with a slope as large as 70 cm^{-1} per unit concentration. This quasilinear behavior can be used to determine the Al concentration in bulk mixed crystals: indeed, the long-range nature of the Coulomb field accompanying the charged particles probes sufficiently deep in the material to give access to the average bulk concentration of Al. We conclude that this method can be used as far as the probing material is thick enough to avoid any interfacial effects and provides concentration values with an accuracy of 5%.

A. Intensities

The intensities of the two main peaks have been measured by the semitheoretical way described above. They correspond to the area under the Lorentzian curves used to generate the first-order loss probability. The left panel of Fig. 6 represents the intensity ratio of the two main peaks. The right panel represents the evolution of their respective and total areas *versus* the Al concentration. We observe a nearly linear evolution of the intensities for Al concentrations between $0.1<x<0.9$. The GaAs-like branch intensity increases more slowly than the AlAs-like one.

For an isotropic material, such as $Al_xGa_{1-x}As$, the classical loss probability, i.e., the angle-resolved loss function integrated over the spectrometer aperture is given by[22]

$$P_{cl}(\omega)=K(E_0,\theta_i,\theta_r,\Psi_a,\omega)\frac{1}{\omega}\mathrm{Im}\frac{-1}{\varepsilon(\omega)+1}\ . \tag{3}$$

This function can be separated in two distinct factors: the first one defines the dipole lobe and appears to be approximately the same for the two oscillators; the second factor contains the surface loss function. Taking for the dielectric function a sum of two Lorentzian oscillators, the surface loss function can be written as

$$\frac{1}{\omega}\mathrm{Im}\frac{-1}{\varepsilon(\omega)+1}\cong\left[\frac{\pi}{2(\varepsilon_\infty+1)}\right]\left\{\frac{(\omega_{\mathrm{TO1}}^2-\omega^2)(\omega_{\mathrm{TO2}}^2-\omega^2)}{(\omega^2-\omega_-^2)\omega^2}\delta(\omega-\omega_+)+\frac{(\omega_{\mathrm{TO1}}^2-\omega^2)(\omega_{\mathrm{TO2}}^2-\omega^2)}{(\omega^2-\omega_+^2)\omega^2}\delta(\omega-\omega_-)\right\}, \tag{4}$$

where ω_- and ω_+ are the two FK mode frequencies and ω_{TO1} and ω_{TO2} are the two TO phonon frequencies associated with the GaAs- and AlAs-like branches, respectively. This formula gives the sum of the two surface loss peak intensities I_- and I_+ for GaAs- and AlAs-like modes, respectively. The total loss probability is obtained by replacing in I_- and I_+, ω_- and ω_+ by the roots of Eq. (2), i.e., by equating the double Lorentzian oscillator dielectric function of $Al_xGa_{1-x}As$ to -1,

$$I_++I_-\cong\frac{\pi}{2(\varepsilon_\infty+1)}\frac{f_1+f_2}{f_1+f_2+\varepsilon_\infty+1}$$

$$=\frac{\pi}{2}\frac{\varepsilon_0-\varepsilon_\infty}{(\varepsilon_0+1)(\varepsilon_\infty+1)}\ . \tag{5}$$

f_1 and f_2 represent the oscillator strengths of the two oscillators. Both together obey the sum rule $f_1+f_2=\varepsilon_0-\varepsilon_\infty$ where ε_0 is the static dielectric constant. Assuming a linear dependence of the static and high-frequency dielectric constants upon Al concentration, we compared the theoretical results (Fig. 6, solid line) to the experimental data. The prefactor $K(E_0,\theta_i,\theta_r,\Psi_a,\omega)$ has been adjusted to fit the data points and was found to be equal to 6. The agreement is reasonable in the sense that the tendency of the total loss area is well reproduced.

The left panel of Fig. 7 displays the oscillator strengths of the GaAs- and AlAs-like modes calculated by using Bonneville's model. In fact, the oscillator strengths of each band are nearly proportional to their corresponding LT splitting. The oscillator strength of the AlAs-like mode exhibits a linear behavior, whereas the GaAs-like mode has a plateau in the Al concentration range between 0.1 to 0.4. The right panel displays the intensity of the AlAs- and GaAs-like surface modes calculated using Eq. (4), and taking the frequencies deduced from the Bonneville's model. We observed that, as expected, the intensities of both peaks exhibit the same behavior as the oscillator strengths, because there exists a high degree of correlation between the oscillator strengths and the respective surface loss intensities. Looking at Fig. 6 (right panel), we can conclude from the evolution of the intensities of both peaks that their respective oscillator strength exhibits the same behavior, i.e., a linear behavior between $x=0.1$ and 0.9. Although the CPA model gives a linear evolution for the AlAs-like mode, the behavior of

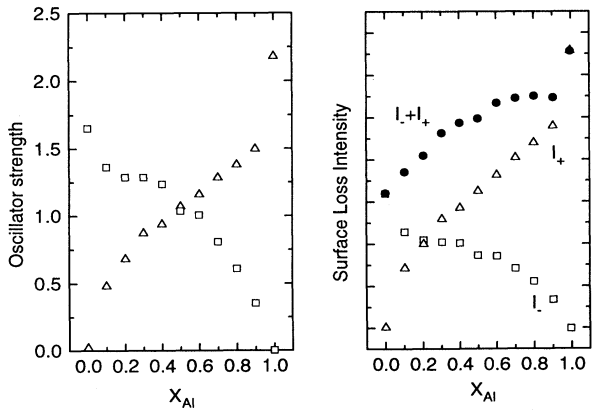

FIG. 7. Left panel: oscillator strengths of the AlAs- and GaAs-like modes vs the aluminum concentration calculated from Bonneville's model. Right panel: intensities of the surface loss peaks calculated using Eq. (4).

the GaAs-like branch is not so well reproduced. The model presented by Baroni, de Gironcoli, and Giannozzi[12] and based on *ab initio* calculations seems to provide a better description of the observed linear variation of the LT splitting of the GaAs-like branch.

B. Theoretical simulation

In principle, the dielectric theory is able to produce a complete HREELS spectrum, provided that one measures in the dipole scattering regime and that the dielectric function of the material is known.[23] We have performed such a calculation with the infrared optical parameters deduced from the Bonneville's model. First-order loss peak areas were determined from the computed spectra. The evolution of these areas versus Al concentration was found to be in good qualitative agreement with the measured values plotted in Fig. 7, however with intensities too low by a factor of 2. Preliminary measurements on pure GaAs and AlAs crystals[24] showed excellent quantitative agreement with the dielectric theory. However, in that case, the spectra were recorded at significantly higher impact energies (5 eV). We have investigated several reasons that could explain this discrepancy.

(a) The "image charge effect." The attraction between the incident electron and its image charge below the surface is not negligible at such low energies.[22] However, it contributes to accelerate the electron and thus induces a reduction of the energy-loss probability. Thus, this correction goes in the wrong direction and cannot be invoked here.

(b) A "resonance" effect. Negative ion resonances are well known from gas-phase measurements and have also been observed by HREELS in physisorbed layers.[25] A similar effect could happen on clean solid surfaces, where the electron could be temporarily trapped in some unoccupied conduction band of the substrate before being emitted, thus enhancing the interaction probability with the surface excitations. Such an effect was reported by Thiry *et al.*[26] on $UO_2(111)$ where resonant scattering from the $5f$ unoccupied bands was observed to enhance the energy-loss intensities. Although a similar mechanism could be invoked to account for the discrepancy in the work presented here, we lack the experimental data in order to proceed further in this discussion. Especially detailed measurements of energy-loss intensities at different impact energies around 3 eV would certainly allow us to disclose the presence of resonant effect in the HREELS spectra. Further theoretical and experimental studies are thus necessary in order to investigate the importance of resonant scattering in the case of GaAs and related ternary alloys.

IV. CONCLUSIONS

In situ grown thick epitaxial $Al_xGa_{1-x}As$ films have been analyzed by HREELS. Two FK surface optical modes (GaAs- and AlAs-like) have been observed. Their frequencies and intensities have been measured by a semitheoretical treatment, over the whole Al concentration range $0<x<1$. The evolution of the frequencies is in keeping with the expected two-mode behavior. The observation of a linear behavior of the optical surface-phonon frequency splitting with the aluminum concentration permits the introduction of a new method of measurements of the Al concentration in such ternary alloys. This method is found to give a precision of the order of 5%. The measured intensities are significantly larger than the values calculated from the dielectric theory. This effect is tentatively explained by some resonant electron scattering at the clean solid surface similar to the well-known negative-ion resonances that have been observed both in gas phase or in physisorbed layers. On the other hand, the evolution of the intensities allows to determine that in the case of $Al_xGa_{1-x}As$, the oscillator strengths of both oscillators vary linearly in the concentration range between $x=0.1-0.9$.

ACKNOWLEDGMENTS

Two of us, R.S. and Ph.L. acknowledge the Belgian National Fund for Scientific Research. We also acknowledge financial support of the Belgian Fund for Joint Basic Research. This work presents research results obtained in the framework of the Belgian National Program of Inter University Attraction Poles initiated by the Belgian State Primer Minister's Office for Science Policy Programming.

[1]M. Ilegems and G. L. Pearson, Phys. Rev. B **1**, 1576 (1970).
[2]R. Tsu, H. Kawamura, and I. Esaki, in *Proceedings of the International Conference on the Physics of Semiconductors,* edited by M. Miasek (PWN-Polish Scientific, Warsaw, 1972), Vol. 2, p. 1135.
[3]G. Abstreiter, E. Bauer, A. Fischer, and K. Ploog, Appl. Phys. **16**, 345 (1978).
[4]B. Jusserand and J. Sapriel, Phys. Rev. B **24**, 7194 (1981).
[5]B. Jusserand, D. Paquet, and F. Mollot, Phys. Rev. Lett. **63**, 2397 (1989).
[6]D. E. Aspnes, S. M. Kelso, P. A. Logan, and R. Bhat, J. Appl. Phys. **60**, 756 (1986).
[7]T. Yuasa, S. Naritsuka, M. Mannoh, K. Shinozaki, K. Yamanaka, Y. Nomura, M. Mihara, and M. Ishii, Phys. Rev. B **33**, 1222 (1986).
[8]D. Kirillov, Y. Chai, C. Webbs, and G. Davis, J. Appl. Phys. **59**, 231 (1986).
[9]I. F. Chang and S. S. Mitra, Adv. Phys. **20**, 359 (1971); Phys. Rev. B **2**, 1215 (1970), and references therein.
[10]A. S. Barker, Jr. and J. R. Sievers, Rev. Mod. Phys. **47**, S1 (1975).
[11]R. Bonneville, Phys. Rev. B **24**, 1987 (1981).
[12]S. Baroni, S. de Gironcoli, and P. Giannozzi, Phys. Rev. Lett. **65**, 84 (1990).
[13]A. A. Lucas and M. Sŭnjić, Prog. Surf. Sci. **2**, 75 (1972).
[14]P. A. Thiry, M. Liehr, J. J. Pireaux, R. Caudano, and T. Kuech, J. Vac. Sci. Technol. **4**, 953 (1986).
[15]A. J. Spring Thorpe, S. J. Ingrey, B. Emmerstorfer, and P.

Mandeville, Appl. Phys. Lett. **50**, 77 (1986).
[16]B. A. Joyce, P. J. Dobson, J. H. Neave, K. Woodbridge, J. Zhang, P. K. Larsen, and B. Bolger, Surf. Sci. **168**, 423 (1986).
[17]P. A. Thiry, M. Liehr, J. J. Pireaux, and R. Caudano, Phys. Rev. B **29**, 4824 (1984).
[18]A. A. Lucas and J. P. Vigneron, Solid. State. Commun. **49**, 327 (1984).
[19]O. G. Lorimor and W. G. Spitzer, J. Appl. Phys. **37**, 2509 (1966).
[20]P. Mazur, E. W. Montroll, and R. P. Potts, J. Wash. Acad. Sci. **46**, 2 (1956).
[21]Sadao Adachi, J. Appl. Phys. **58**, 1 (1985).
[22]A. A. Lucas, J. P. Vigneron, Ph. Lambin, P. A. Thiry, M. Liehr, J. J. Pireaux, and R. Caudano, Int. J. Quant. Chem. **19**, 687 (1986).
[23]Ph. Lambin, J. P. Vigneron, and A. A. Lucas, Phys. Rev. B **32**, 8203 (1985).
[24]A. Degiovanni, J.-L. Guyaux, P. A. Thiry, and R. Caudano, Surf. Sci. **251-2**, 238 (1991).
[25]See the recent review by R. E. Palmer and P. J. Rous, Rev. Mod. Phys. **64**, 383 (1992).
[26]P. A. Thiry, J. J. Pireaux, R. Caudano, J. R. Naegele, J. Rebizant, and J. C. Spirlet, J. Chem. Soc. Faraday Trans. **83**, 1229 (1987).